ISBN: 978-3-95450-231-8 ISSN: 2673-5490 doi: 10.18429/JACoW-IPAC2023-TUPL170

MODELING OF STANDING WAVE RF CAVITIES FOR TRACKING THROUGH MULTI-PASS ENERGY RECOVERY LINAC

C. Guyot*, C. Bruni, A. Fomin, J. Michaud, L. Perrot, W. Kaabi
Université Paris-Saclay, CNRS/IN2P3, IJCLab
S.A. Bogacz† Jefferson Lab, Newport News, USA

Abstract

Short bunches, high current and multiple linac pass are all characteristics of Energy Recovery Linacs (ERLs), which may result in collective effects. They in turn, may affect the beam, degrading its quality, or even yield to instabilities causing a beam loss. To study and mitigate these effects one needs a numerical simulation code, that can take into account both the collective effects, as well as, particular ERL features, such as a multi-turn design that does not reach a steady state or the multiple passages of the beam through RF cavities at different energies. CODAL, a code developed by SOLEIL in collaboration with IJCLab, enables such studies. It is a 6 dimensional (6D) tracking code applying kicks based on the integration of the local Hamiltonian for each element of the lattice. It is also capable of simulating space charge, wake-fields and coherent synchrotron radiation.
However, to correctly take into account the ERL dynamics, an upgrade had to be made to include the effect of a standing wave Radio-Frequency (RF) cavity in 6D. In this paper, we will concentrate on the implementation and benchmarking (with DESY's tracking code ASTRA) of both the longitudinal and the transverse models (by J.B. Rosenzweig and L. Serafini), which we use to carry out tracking of fully analytical 6D RF cavity.

INTRODUCTION

The ERLs rely on the fact that the energy transfer from the RF wave to the particles is a reversible process. This potentially allows one to recover most of the beam energy through transfer to the RF field, which may be used to accelerate the next beam bunches [1].

An ERL can be seen as a hybrid accelerator, which is neither a linear accelerator nor a storage ring, thus it is subject to constraints from both. From the longitudinal point of view, the energy spread needs to be controlled in order to avoid strong chromatic effects in the arcs, which would cause an emittance increase. As is well known, non-linearity of the longitudinal phase-space can lead to a strong emittance degradation, and may be a seed of the micro-bunching instability triggered by coherent synchrotron radiation effects. The non-linear longitudinal effect of the accelerating cavities may enhance the micro-bunching instability threshold. In addition, accelerating cavities should be properly modeled to include the transverse focusing effects in the accelerating mode and defocusing effects in the decelerating one. This transverse effects will affect the Twiss parameters, which will impact the optical design of arcs. For these reasons, accelerating cavities have to be accurately modeled from the longitudinal and transverse points of view.

* coline.guyot@ijclab.in2p3.fr
† This work is supported by U.S. Department of Energy under DE-AC05-06OR23177.

ANALYTICAL MODELS

Combining two existing models, a fully analytic 6D tracking can be used to simulate the effect of standing wave RF cavity on beam dynamics for ERL start-to-end simulation including collective effect studies. The use of a fully analytic model should facilitate faster simulations, while still including all relevant physical effects due to the RF cavities.

Longitudinal Model

For the relative longitudinal position calculation, we assume potential off-axis effects to be negligible, leaving the dynamics to be dominated by off-momentum differences, as it can be seen in Eq. (1).

$$s_f = s_i + \frac{\delta\ L}{\gamma_i^2} \tag{1}$$

with s the particle relative position (labeled by the index 'i' before the cavity and 'f' after it), L is the cavity length and γ_i denotes the Lorentz Factor at the entrance.

An analytical calculation of the energy gain for a standing wave cavity can be carried out from the accelerating field E_z by considering $\frac{dE}{dt} = \frac{dE}{dz}\frac{dz}{dt} = \vec{F}.\vec{v} = e\,E_z$ [2]. Assuming that the particle phase is constant across the cavity, we obtain:

$$\begin{aligned}\mathscr{E}_f = \mathscr{E}_i + \frac{V_{rf}}{L}[\frac{1}{2k}cos(\phi(s)) \\ - \frac{1}{2k}cos(2kL + \phi(s)) + sin(\phi(s))L]\end{aligned} \tag{2}$$

where $\phi(s) = \phi_{syn} - ks$ is the particle phase, ϕ_{syn} is the synchronous phase, V_{rf} is the optimal energy gain, and k represents the RF wave-number.

Equation (2), is then used to find the normalized relative energy spread values:

$$\delta_f = \frac{(1+\delta_i)\mathscr{E}_f(s) - \mathscr{E}_{f,syn}(s)}{\mathscr{E}_{f,syn}(s)} \tag{3}$$

Transverse Model

Even if the main effect of RF cavity results from the longitudinal dynamics, the transverse effects can still be of importance. Sensitivity to the transverse effects mainly depends on the energy and the accelerating gradient, so that

Content from this work may be used under the terms of the CC BY 4.0 licence (© 2022). Any distribution of this work must maintain attribution to the author(s), title of the work, publisher, and DOI.

ISBN: 978-3-95450-231-8 ISSN: 2673-5490 doi: 10.18429/JACoW-IPAC2023-TUPL170

© Content from this work may be used under the terms of the CC BY 4.0 licence (© 2022). Any distribution of this work must maintain attribution to the author(s), title of the work, publisher, and DOI.

for lower energies or higher gradients the particle motion will be more affected.

As the electron propagates, it will see the entrance fringe field, then the acceleration structure field, and finally a fringe field at the exit. As these are different effects happening at a different positions, they are derived separately (similarly to an analytic derivation for magnets).

This is the approach taken by the well-tested model developed by J.B. Rosenzweig and L. Serafini [3, 4], which was chosen here. The transverse forces due to the accelerating field are calculated from the longitudinal acceleration field expression. To analytically obtain the average motion a few approximations are done. The derivation works for relativistic electrons with cylindrical symmetry. The average motion is then derived for a fringe field (see Eq. (4)) and for one accelerating gap (see Eq. (5)).

The fringe field matrices $M_{entrance/exit}$ of a cavity are:

$$\begin{bmatrix} 1 & 0 \\ \mp\frac{\gamma'}{2\gamma_{i/f}} & 1 \end{bmatrix} \tag{4}$$

The combination of both fringe fields will have an overall focusing effect for an accelerating pass, while it will cause defocusing for a decelerating one.

For the accelerating gap, the average transverse motion expression is derived using additional approximations, assuming a smooth evolution of both the transverse position and the Lorentz factor. This requires that for multi-cell cavities, each accelerating gap has to be considered separately to ensure that these variations remain small. The Matrix M_{cell} is expressed as:

$$\begin{bmatrix} \cos(\alpha) & \sqrt{\frac{8}{\eta(\phi)}}\frac{\gamma_i}{\gamma'}\cos(\Delta\phi)\sin(\alpha) \\ -\sqrt{\frac{\eta(\Delta\phi)}{8}}\frac{\gamma'\sin(\alpha)}{\gamma_f\cos(\Delta\phi)} & \frac{\gamma_i}{\gamma_f}\cos(\alpha) \end{bmatrix} \tag{5}$$

$\Delta\phi$ is the phase difference, $\alpha = \frac{\sqrt{\eta(\Delta\phi)/8}}{\cos(\Delta\phi)} ln(\frac{\gamma_f}{\gamma_i})$, $\eta = \sum_{n=1}^{\infty} b_n^2 + b_{-n}^2 + 2b_n b_{-n}\cos(2\Delta\phi)$, γ is the Lorentz factor and $\gamma' = \frac{E_{acc}}{m_e c^2}\cos(\Delta\phi)$, where E_{acc} is the mean accelerating gradient.

BENCHMARKING

The analytical models presented here have been implemented in a 'homemade' code call CODAL [5], which has been used the obtain simulation results shown here. The validation of the code upgrade is done comparing the results with the well-known code ASTRA [6]. The ASTRA tracking through RF cavities has been carried out using the standing wave mode and a longitudinal on-axis accelerating cavity field extracted from an electromagnetic solvers. This choice provides two major advantages. First, the approach is complementary to an analytical model, as ASTRA resolves the equation of motion using a direct numerical integration based on the Runge-Kutta method. Secondly, as a code renown for properly taking into account low energy effects, it is a tool that allows one to confirm, whether the approximations of the analytical model are adapted to the studies even at their lowest energy.

The plots presented here will illustrate one example (which corresponds to the first accelerating section of a multipass high current ERL demonstrator project, PERLE [7]). A 6D Gaussian beam generated by ASTRA (see Table 1) passes through four 5-cells standing wave RF cavities, going from 7 up to 89 MeV. The energy transfer is assumed to be on crest with a 20.54 MeV energy gain per cavity. All cavities have a length of 93.5 cm and operate at a frequency of 801.58 MHz.

Table 1: Simulation 6D Gaussian Beam Initial Parameters

Parameter	**Value**	**Unit**
Nominal Energy $\mathscr{E}_n$	7.0	MeV
Normalized Energy Spread σ_δ	0.01	%
Longitudinal Size σ_s	3.0	mm
Transverse Size $\sigma_{x/y}$	0.89	mm
Divergence $\sigma_{x'/y'}$	0.45	mrad
Transverse Normalized Emittance $\epsilon_{n,x/y}$	0.9	mm.mrad
Charge	500	pC
Twiss Parameter β	11.7	
Twiss Parameter α	5.8	

Longitudinal Dynamics

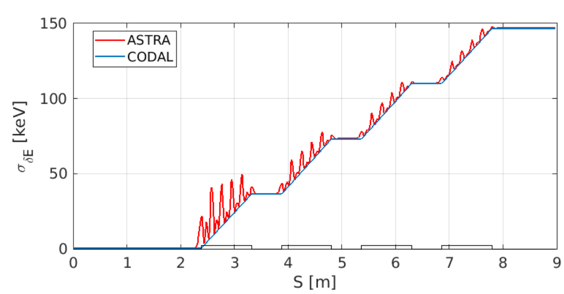

Figure 1: Simulated rms energy spread $\sigma_{\delta E}$ [keV] along a four RF cavities section for both ASTRA (Runge-Kutta integration) and CODAL (analytical model). The initial Gaussian beam is used, as described in Table1.

.

The evolution of standard deviation of the normalized energy spread $\sigma_{\delta E}$ [keV] ($\delta E = \mathscr{E} - \mathscr{E}_n$) along a section with 4 cavities is plotted in Fig. 1. Considering the time step for the resolution in ASTRA, an oscillatory motion in the cavity can be seen, whereas the kick model only represents the average motion between the entry and the exit of the cavity. Nevertheless, the resulting plots are in good agreement.

For adequate beam dynamics studies, it is essential to have access to a more detailed evolution of the beam through its 6D distributions and phase-space. For example, the longitudinal charge density is one of the critical variables for

ISBN: 978-3-95450-231-8 ISSN: 2673-5490 doi: 10.18429/JACoW-IPAC2023-TUPL170

Coherent Synchrotron Radiation (CSR) effect. Therefore, it is necessary to also ensure the analytic model remains representative on this level. This is apparently the case, as it can be seen in the example illustrated in Fig. 2.

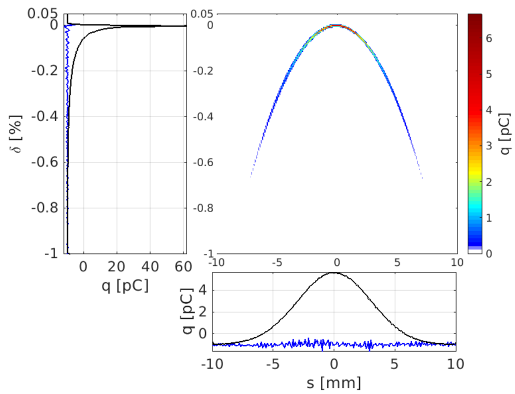

Figure 2: Simulated longitudinal phase-space (δ, s) [%, mm] at the end of the accelerating section (at 8.97 m) from CODAL and associated projections *(in black)*, as well as 10 times the projection differences between ASTRA and CODAL *(in blue)*.

Figure 2 illustrates the longitudinal phase-space, as well as the associated projection *(black line)* and 10 times the discrepancy between Astra and Codal ($projection_{Astra} - projection_{Codal}$)x10 in pC). The discrepancy is at most of a few percent, which shows a good agreement between the two methods.
As ASTRA is suitable for simulation of low energy electron beams and resolves the motion from the accelerating field on axis, the standing wave cavity module enables to take into account phase slippage effects as well as potential path-length difference due to initial transverse characteristic difference. The agreement with the ASTRA simulations proves the validity of the approximations made in the analytical model for the PERLE studies.

Transverse Dynamics

Evolution of both the transverse beam size and its divergence after passing though four RF cavities, represented in Fig. 3, reveals the beam 'sees' an overall focusing effect by the accelerating cavity fields. Furthermore, evolution of the root mean square (rms) divergence shows it even more clearly with a value divided by an order of magnitude after passing through 4 cavities. It can also be seen from the rms sizes. Even if the beam size is still increasing with a beam that remains divergent, the slopes at the exit of the cavities have decreasing values. At the end of the section, the divergence difference is of 0.34% with $\sigma_{x',Codal} = 0.0290\ mrad$ and $\sigma_{x',Astra} = 0.0289\ mrad$, while the size at 8.97 m is $\sigma_{x,Codal} = 0.322\ mm$ and $\sigma_{x,Astra} = 0.317\ mm$, corresponding to a 1.55% difference.

The transverse phase-space (x', x) resulting from CODAL simulation is shown in Fig. 4 with their projections in pC *(black line)* and the associated 10 times the discrepancy

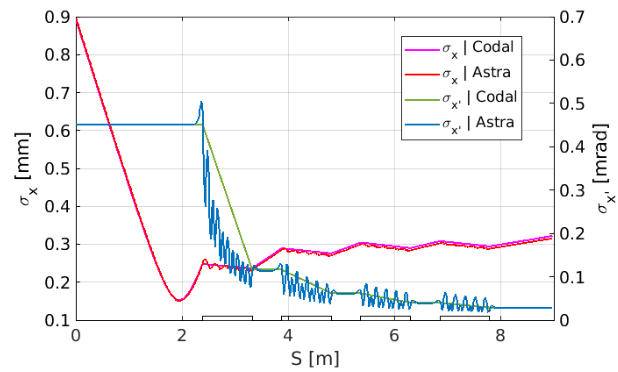

Figure 3: Simulated rms transverse horizontal size σ_x *(left axis)* and rms horizontal divergence $\sigma_{x'}$ *(right axis)* along a four RF cavities section for both ASTRA (Runge-Kutta integration) and CODAL (analytical model)

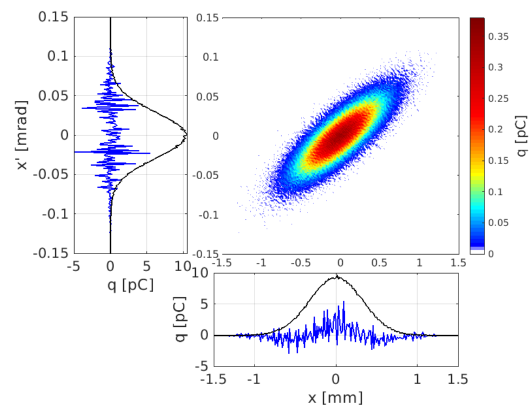

Figure 4: Simulated Transverse phase-space (x', x) [mrad,mm] at the end of the accelerating section (at 8.97 m) from CODAL and associated projections *(in black)* as well as 10 times the projection differences between Astra and CODAL *(in blue)*.

between ASTRA and CODAL. The conditions of validity of the analytical model has been fully confirmed as being well adapted and adequate when there is a separate application of the fringe fields at the entrance and exit and the purely accelerating gap matrix for each cell of the RF cavity. Finally, it shows that the decoupling of motion in all 3 directions is a realistic hypothesis for the simulation of the cavities.

CONCLUSION

To properly simulate beam dynamics of multi-pass, high current ERLs one needs to include collective effects combined with higher order, 6D tracking in the arcs and accelerating cavities. Combining these two analytic methods is critical to obtain an adequate picture of both the longitudinal and transverse beam dynamics. For a standing wave RF cavity the model enables efficient simulation, which has been confirmed by a comparison with this different numerical approach, tracking with ASTRA.

Content from this work may be used under the terms of the CC BY 4.0 licence (© 2022). Any distribution of this work must maintain attribution to the author(s), title of the work, publisher, and DOI.

ISBN: 978-3-95450-231-8 ISSN: 2673-5490 doi: 10.18429/JACoW-IPAC2023-TUPL170

Content from this work may be used under the terms of the CC BY 4.0 licence (© 2022). Any distribution of this work must maintain attribution to the author(s), title of the work, publisher, and DOI.

REFERENCES

[1] M. Tigner, "A possible apparatus for electron clashing-beam experiments", *Il Nuovo Cimento (1955-1965)*, vol. 37, pp. 1228–1231, Jun. 1965. doi:10.1007/BF02773204

[2] T. Vinatier, "Influence des paramètres du laser sur la dynamique des paquets courts d'électrons relativistes dans des accélérateurs linéaires basés sur des canons RF et développement de diagnostics associés", Ph.D. thesis, Physique Paris 11, 2015.

[3] J. B. Rosenzweig and L. Serafini, "Transverse particle motion in radio-frequency linear accelerators", *Phys. Rev. E*, vol. 49, pp. 1599–1602, Feb. 1994. doi:10.1103/PhysRevE.49.1599

[4] S. Reiche *et al.*, "Experimental confirmation of transverse focusing and adiabatic damping in a standing wave linear accelerator", *Phys. Rev. E*, vol. 56, no. 3, pp. 3572-–3577, Sep 1997. doi:10.1103/PhysRevE.56.3572

[5] A. Gamelin, "Collective effects in a transient microbunching regime and ion cloud mitigation in ThomX", Theses, Université Paris-Saclay, September 2018.

[6] K. Floettmann, "ASTRA: A space charge tracking algorithm documentation", DESY, Hamburg, Germany, 1997, http://www.desy.de/~mpyflo/

[7] D. Angal-Kalinin *et al.*, "PERLE. Powerful energy recovery linac for experiments. Conceptual design report", *J. Phys. G: Nucl. Part. Phys.*, vol. 45, no. 6, p. 065003, May 2018. doi:10.1088/1361-6471/aaa171